Interaction of Unfused Tricyclic Aromatic Cations with DNA: A New Class of Intercalators†

W. David Wilson,* Farial A. Tanious, Rebecca A. Watson, Henryk J. Barton, Alewtina Strekowska, Donald B. Harden, and Lucjan Strekowski*

Department of Chemistry and Laboratory for Microbial and Biochemical Sciences, Georgia State University, Atlanta, Georgia 30303

Received August 17, 1988; Revised Manuscript Received October 28, 1988

ABSTRACT: Unfused tricyclic aromatic ring systems **1–6** with one or two cationic side chains have been synthesized and their interactions with DNA and synthetic polymers probed with a variety of techniques. Molecular mechanics calculations indicate that the torsional angle between ring planes in the minimum energy conformation of the tricyclic molecules can range from 0° to as high as 50° depending on the type of rings and substituents. Viscometric titrations with linear and supercoiled DNA, linear dichroism, and NMR studies indicated that all compounds with torsional angles of approximately 20° or less bind to DNA by intercalation. The more highly twisted intercalators caused significant perturbation of DNA structure. Unfused intercalators with twist angles of approximately 20° have reduced binding constants, suggesting that they could not form an optimum interaction with the DNA base pairs. Unfused intercalators with twist less than 20° formed strong complexes with DNA. The structures of these unfused intercalators are more analogous to typical groove-binding molecules, and an analysis of their interaction with DNA provides a better understanding of the subtle differences between intercalation and groove-binding modes for aromatic cations. The results indicate that intercalation and groove-binding modes should be viewed as two potential wells on a continuous energy surface. The results also suggest design strategies for intercalators that can optimally complement DNA base pair propeller twist or that can induce bends in DNA at the intercalation site.

The design and synthesis of intercalators, groove-binding molecules, oligopeptides, and oligonucleotide single strands that can selectively recognize base pairs, sequences, and/or conformational features of nucleic acids are areas of importance and intense interest [cf. Dervan (1986), Goodsell and Dickerson (1986), Helene et al. (1985), Hurley and Boyd (1987), Langaa et al. (1985), Lee et al. (1988), Moser and Dervan (1987), Neidle et al. (1987), Palmer et al. (1988), Pullman (1987), Strekowski et al. (1988a,b), Wakelin (1986), Wilson et al. (1985b, 1988), and Zimmer and Wahnert (1986)]. By far the most research has been conducted on the interactions of intercalators and groove-binding molecules with DNA.[1] Molecules that bind by these two different mechanisms can be divided into two different general structural classes (Waring, 1981; Wilson, 1989).

Intercalators are typically fused-ring, planar aromatic molecules with cationic charges and/or cationic groups attached to the intercalating ring (Wilson & Jones, 1981). Groove-binding molecules, on the other hand, generally contain a sequentially linked array of small, nonfused aromatic systems linked by groups or bonds with potential torsional freedom (Zimmer & Wahnert, 1986). They also usually contain cationic groups with the basic functions at one or both ends of the molecule. The bithiazoles of bleomycin have been proposed as an intermediate type of intercalation system; however, there is no general agreement as to whether the bithiazoles bind by intercalation or groove interactions when they are a part of the bleomycin molecule (Stubbe & Kozarich, 1987).

The antibiotic actinomycin D is another example of a molecule with an intermediate type of binding interaction. The molecule is neutral and has an intercalating phenoxazone ring system (Waring, 1981). The binding free energy and specificity for GC sequences are, however, largely supplied by two large cyclic peptides that bind in the DNA minor groove (Ginell et al., 1988).

The distinction between intercalators and groove-binding molecules may be quite subtle, however. For example, it is known that most intercalators, at high ratios of compound to DNA base pairs, bind in an external, electrostatically stabilized complex (Wilson & Jones, 1981). On the other hand, many groove-binding molecules are approximately planar or could become planar with a small expenditure of energy. The structure of these molecules suggests that they could intercalate in the same manner as planar cations if the favored groove-binding interaction could be inhibited (Wilson, 1989).

The base pairs of DNA are held together by hydrogen bonds and can have significant propeller twist (Calladine, 1982; Dickerson, 1983; Tung & Harvey, 1986). It would seem possible to design twisted-unfused aromatic systems that could complement the propeller twist of base pairs. One of our goals in designing bleomycin amplifiers, molecules that significantly increase the rate of bleomycin-catalyzed cleavage of DNA

† This work was supported by NSF Grant DBM-8603566 (W.D.W.), American Cancer Society Grant CH383 (L.S.), the donors of the Petroleum Research Fund, administered by the American Chemical Society (L.S.), Greenwall Foundation, Inc., Grant of Research Corporation (L.S.), and NIH Grant SO7-RR07171 (W.D.W. and L.S.). The 400-MHz NMR spectrometer was obtained with partial support from a departmental NSF grant.

[1] Abbreviations: DNA, deoxyribonucleic acid; EDTA, ethylenediaminetetraacetic acid; PIPES, piperazine-*N*,*N*′-bis[2-ethanesulfonic acid]; d(A-T)$_2$, poly[d(A-T)]·poly[d(A-T)]; d(G-C)$_2$, poly[d(G-C)·poly[d(G-C)]. The conformation of a heterobiaryl [s-cis (cisoid) or s-trans (transoid)] is determined by a spatial relationship between two heteroatoms of each ring, nearest to the inter-ring bond.

0006-2960/89/0428-1984$01.50/0

Scheme I

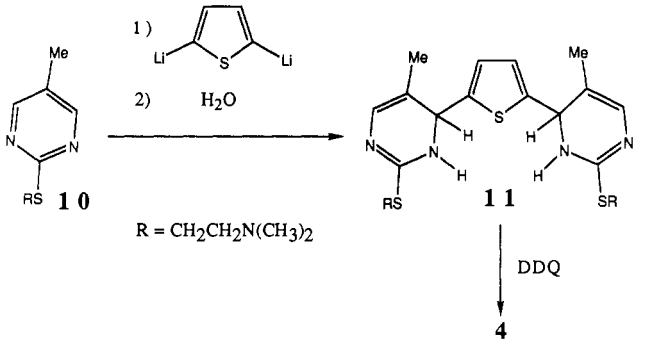

(Brown & Grigg, 1982), was to prepare a series of twisted, nonfused, aromatic cations that could match or enhance base-pair propeller twist and bind to DNA by intercalation. Several studies have suggested that molecules of this type have good amplification activity (Strekowski et al., 1986a, 1987, 1988a).

We have previously shown that **1** (Figure 1) is both an intercalator and a bleomycin amplifier (Wilson, 1989; Wilson et al., 1988). Crystallographic and molecular modeling have indicated that the two phenyl rings of **1** are twisted out of the pyrimidine plane by approximately 20° due to steric clash of protons on the phenyl and pyrimidine rings. With **2** (Figure 1) the twist is approximately 45–50°, and it binds by a groove interaction with a significantly lower binding constant than **1** (Wilson, 1989; Wilson et al., 1988). Preliminary studies have shown that **3** intercalates strongly with DNA (Strekowski et al., 1987). To probe the binding mechanism of such nonfused ring compounds in more detail, we have now synthesized the aromatic cations **4–6** and studied the interactions of **3–6** with natural DNA and synthetic polydeoxyribonucleotides. All four of these compounds bind to DNA by intercalation. The strongest intercalation binding of **1–6** is obtained with **3**, which is particularly interesting given its close structural similarity to the groove-binding molecule 4′,6-diamidino-2-phenylindole (DAPI, **9** in Figure 1) and other groove-binding molecules. As a result of these studies, design strategies for molecules that specifically recognize base-pair propeller twist and that can cause bends at an intercalation binding site are proposed.

Materials and Methods

4,6-Bis[4′-[[2″-(dimethylamino)ethyl]thio]phenyl]pyrimidine (**1**), 4,6-bis[4′-[[2″-(dimethylamino)ethyl]thio]-phenyl]-5-methylpyrimidine (**2**) (Wilson et al., 1988), 2,5-bis[2′-[[2″-(dimethylamino)ethyl]thio]pyrimidin-4′-yl]-thiophene (**3**) (Strekowski et al., 1987), *N,N*-dimethyl-2-[(4′-thien-2″-ylpyrimidin-2′-yl)thio]ethylamine (**7**), *N,N*-dimethyl-2-[(5′-methyl-4′-thien-2″-ylpyrimidin-2′-yl)thio]-ethylamine (**8**), and *N,N*-dimethyl-2-[(5′-methylpyrimidin-2′-yl)thio]ethylamine (**10**) (Strekowski et al., 1988a) were prepared as described.

2,5-Bis[2′-[[2″-(dimethylamino)ethyl]thio]-5′-methylpyrimidin-4′-yl]thiophene (**4**). Compound **4** was obtained as shown in Scheme I. A solution of *n*-butyllithium in hexane (1.8 M, 1.64 mL, 2.94 mmol) was added dropwise to a stirred solution of 2,5-dibromothiophene (356 mg, 1.47 mmol) in dry ethyl ether (50 mL) at −40 °C under a nitrogen atmosphere. After the addition was complete, stirring was continued for an additional 20 min, and the resultant solution of 2,5-dilithiothiophene was treated dropwise at −40 °C with a solution of **10** (645 mg, 3.27 mmol) in ethyl ether (10 mL). The mixture was stirred at −40 °C for 30 min and then at 23 °C for 30 min, quenched with water (1 mL), and treated with a

Scheme II

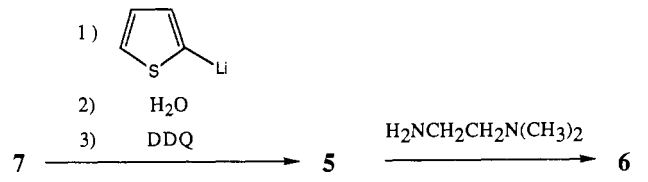

solution of 2,3-dichloro-5,6-dicyanobenzoquinone (DDQ, 742 mg, 3.27 mmol) in tetrahydrofuran (10 mL) to aromatize the intermediate dihydro derivative **11**. The mixture was refluxed for 10 min and then stirred with an aqueous solution of NaOH (10%, 25 mL). The organic layer was separated, dried with Na_2SO_4, and concentrated. Chromatography on silica gel (hexanes/triethylamine, 2/8) was followed by crystallization from hexanes to give 209 mg (30%) of **4**: mp 134–134.5 °C. Anal. Calcd for $C_{22}H_{30}N_6S_3$: C, 55.67; H, 6.37. Found: C, 55.55; H, 6.37.

2-[[2″-(Dimethylamino)ethyl]thio]-4,6-di(thien-2′-yl)pyrimidine (**5**). Compound **5** was obtained as shown in Scheme II. A solution of 2-thienyllithium (4.0 mmol) in ethyl ether (30 mL) [generated in the reaction of *n*-butyllithium with thiophene according to the method of Brown et al. (1982)] was treated dropwise with a solution of **7** (1.01 g, 3.8 mmol) in ethyl ether (2 mL) at −35 °C under a nitrogen atmosphere. The mixture was allowed to react and then worked up as described above to furnish 1.12 g (85%) of **5**: mp 108.5–109.5 °C (from methanol). Anal. Calcd for $C_{16}H_{17}N_3S_3$: C, 55.30; H, 4.93. Found: C, 55.22; H, 4.94.

N-[2″-(Dimethylamino)ethyl]-4,6-di(thien-2′-yl)pyrimidin-2-amine Dihydrobromide (**6·2HBr**). A mixture of **5** (1.00 g, 2.88 mmol) and *N,N*-dimethylethylenediamine (10 mL, 91 mmol) was heated in a Parr bomb at 165 °C for 9 h (Scheme II). The excess of the diamine was removed by distillation, and the residue of crude **6** was purified by silica gel chromatography (hexanes/triethylamine, 7/3) to give an oil. This was dissolved in ethanol (10 mL), and the solution was treated with hydrobromic acid (48%, 0.5 mL, 4.4 mmol). The mixture was refluxed briefly and cooled to precipitate a dihydrobromide of **6**. An additional crystallization from ethanol afforded 1.02 g (73%) of **6**·2HBr: mp 255–270 °C (dec). Anal. Calcd for $C_{16}H_{18}N_4S_2$·2HBr: C, 39.04; H, 4.09. Found: C, 39.13; H, 4.18.

DNA Samples. Natural DNA and synthetic polymers were sonicated and purified as previously described (Wilson et al., 1985a,b). DNA samples were dissolved in and dialyzed against the desired buffer for each experiment.

Buffers. PIPES buffers were adjusted to pH 7 and contained 0.01 M PIPES and 10^{-3} M EDTA with NaCl added to give the desired ionic strength: PIPES 00, no added NaCl; PIPES 05, 0.05 M NaCl; PIPES 10, 0.10 M NaCl; PIPES 20, 0.20 M NaCl. For NMR experiments in D_2O a phosphate buffer was used: 0.015 M NaH_2PO_4, 10^{-4} M EDTA, and 0.10 M NaCl, pH 7.

Methods. Procedures for viscometric titrations (Jones et al., 1980), flow dichroism (Banville et al., 1986), and spectrophotometric binding (Wilson et al., 1985a) measurements have recently been presented. Details are given in the figure legends and tables.

NMR. ^1H NMR spectra in 99.96% D_2O–phosphate buffer were obtained with a Varian VXR-400 spectrometer. Samples of **1**, **2**, **5**, and **6** (1.0 mM) and **3** and **4** (0.36 mM) were lyophilized twice from 99.8% D_2O and transferred to a 5-mm NMR tube with 99.96% D_2O. Typical conditions for spectra obtained on the Varian 400 spectrometer include 65 °C, 2000 scans, 2-s pulse repetition rate, 4000-Hz spectral width, 16K

data points, 0.7-mL sample volume, and TSP reference. The low concentrations and high temperatures were used to minimize ligand self-association in the unbound state. Samples were diluted and spectra obtained at 65 °C until chemical shifts were consistent. DNA titrations were then conducted as previously described (Wilson et al., 1985b).

^{1}H NMR spectra of DNA imino protons were obtained on the JEOL GX-270 spectrometer using a Redfield 21412 pulse sequence under the following conditions: 35 °C, 2000 scans, 0.4-s pulse repetition rate, carrier frequency at 13.5 ppm, 8K data points, TSP reference, 10000-Hz spectral width, 10% D_2O in H_2O–phosphate buffer, 20 mM DNA phosphate molarity, and 0.8-mL sample volume in a 5-mm NMR tube.

^{31}P NMR spectra were obtained at 109.25 MHz with the JEOL GX-270 spectrometer under the following conditions: 60 °C, 5000 scans, 45° pulse width, 4.05-s pulse repetition rate, broad-band bilevel decoupling, 8K data points, trimethyl phosphate reference, 2000-Hz spectral width, 10% D_2O in H_2O–phosphate buffer, 20 mM DNA phosphate molarity, and 0.8-mL sample volume in a 5-mm NMR tube inserted into a 10-mm NMR tube filled to the sample volume level with 99.8% D_2O buffer.

Molecular Modeling. Molecular mechanics calculations (Burket & Allinger, 1982) were conducted on a MicroVax II as previously described (Wilson et al., 1988) using the program Macromodel 2.0 supplied by Professor Clark Still of Columbia University. Conformational analysis was performed on an Evans and Sutherland PS390 molecular graphics terminal using Macromodel 2.0.

Results

Structures of **1–6.** Energetically optimum torsional angles and both the barriers to rotation and shapes of the potential energy–torsional angle function for the unfused aromatic ring systems of **1–6** are critical features for the ability of these compounds to form complexes with DNA. With the simple unfused bicyclic aromatic ring system of biphenyl, X-ray crystallographic results have indicated a coplanar conformation for the two rings of this molecule (Trotter, 1961; Hargreaves et al., 1962). Spectroscopic measurements in solution for several derivatives of this compound, however, have suggested an optimum torsional angle of approximately 35° between the two ring planes [cf. d'Annibale et al. (1973), Field et al. (1977), Field and Sternhell (1981), and Sinton et al. (1984)]. Our molecular mechanics calculations are in excellent agreement with these spectroscopic results and indicate an angle of 36° between the two biphenyl ring planes. Energies of the molecule increase by approximately 2 kcal in both the planar (0°) and perpendicular (90°) orientations of the two rings. Previous X-ray crystallographic and molecular mechanics calculations on **1** and **2** are in good agreement and indicate that the torsional angles between the phenyl and pyrimidine ring planes are approximately 20° in **1** and 50° in **2** (Wilson et al., 1988). The packing forces in the crystal of **1** are apparently not strong enough to force the molecule into a planar conformation as observed with biphenyl. The smaller torsional angle of **1** relative to biphenyl in solution is expected, however, due to the reduced steric clash of protons on the phenyl–pyrimidine rings of **1** relative to the two phenyl rings of biphenyl. The added methyl substituent of **2** again increases the steric interactions, and the torsional angle increases to 50°.

Compounds **3–6** all contain an identical structural core composed of a bicyclic pyrimidine–thiophene ring system substituted with a cationic side chain at the same position. Compounds **3** and **4** have an additional substituted pyrimidine

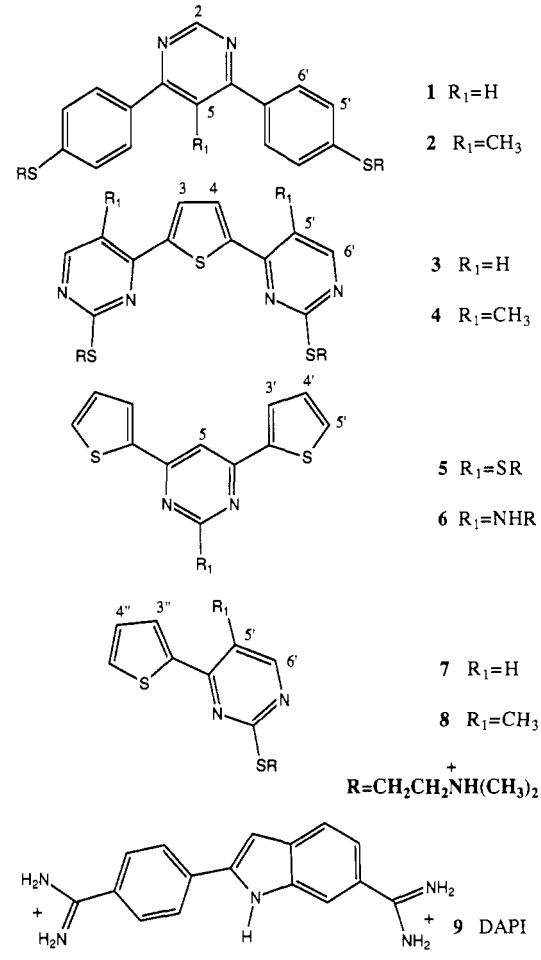

FIGURE 1: Structures for the tricyclic compounds **1–6**, the bicyclic compounds **7** and **8**, and the minor groove binding agent DAPI **9**. Predicted torsional angles for **1–6** based on X-ray crystallographic and molecular modeling results are 0° for **3**, **5**, and **6** and approximately 10° for **4**, 20° for **1**, and 50° for **2**.

system attached to the thiophene ring, while **5** and **6** have an additional thiophene ring substituent on the core pyrimidine ring. **4** has additional methyl substituents at the 5′ positions of the pyrimidine rings. The conformation of all of these compounds depends on the torsional angle between their pyrimidine and thiophene ring planes.

Previous spectroscopic and modeling studies on the bicyclic compound **7** (Figure 1), which constitutes the common structural entity of **3–6**, have shown that the pyrimidine and thiophene rings are coplanar and are in the s-cis[1] conformation as drawn in Figure 1 (Strekowski et al., 1986a,b, 1987, 1988a). On the basis of these results, all three rings of **3**, **5**, and **6** should be in the same plane. Molecular mechanics calculations support this conclusion. We have obtained an X-ray crystallographic structure for the thienylpyrimidine **8** (Figure 1), the bicyclic analogue of **4** (Strekowski et al., 1988b). The unit cell contains three molecules in conformations with a 5–8° twist between the pyrimidine and thiophene rings. Proton NMR NOE experiments in solution on both **4** and **8** indicate that the favored conformation is s-cis with a low torsion angle between the thiophene and pyrimidine rings. We thus expect **4** and **8** to have a similar twist between the aromatic ring planes. Molecular mechanics calculations on **4** predict a torsional angle between the pyrimidine and thiophene rings of 23° but with a low rotational barrier. The energy difference between the optimum torsional angle and the planar orientation, for example, is only approximately 1 kcal/mol. The conformation with a 90° torsional angle is over 3 kcal/mol

Table I: Chemical Shifts and Changes in Chemical Shifts Induced by DNA for **1–6**[a]

compd		H2	H5	H2′,H6′	H3′,H5′	H2″,H3″	$N(CH_3)_2$
1	no DNA	9.16	8.25	8.08	7.64	3.38	2.86
	Δδ	−0.51	−0.48	−0.41	−0.41	−0.03	−0.03
compd		H2	CH_3	H2′,H6′	H3′,H5′	H2″,H3″	$N(CH_3)_2$
2	no DNA	9.03	2.29	7.66	7.66	3.40	2.89
	Δδ	−0.06	−0.02	−0.04	−0.04	0.00	+0.01
compd		H3,H4	H5′	H6′	H2″,H3″	$N(CH_3)_2$	
3	no DNA	7.93	7.59	8.59	3.55	2.95	
	Δδ	−0.76	−0.72	−0.47	−0.12	+0.01	
compd		H3,H4	CH_3	H6′	H2″,H3″	$N(CH_3)_2$	
4	no DNA	7.82	2.49	8.45	3.50	2.92	
	Δδ	−0.54	−0.38	−0.40	−0.07	−0.01	
compd		H5	H3′	H4′	H5′	H2″,H3″	$N(CH_3)_2$
5	no DNA	7.89	8.00	7.31	7.79	3.61	2.98
	Δδ	−0.90	−0.75	−0.55	−0.56	−0.30	−0.09

compd		H5	H3′	H4′	H5′	H2″	H3″	$N(CH_3)_2$
6	no DNA	7.53	7.94	7.29	7.73	3.90	3.50	3.00
	Δδ	−0.84	−0.75	−0.60	−0.60	−0.27	−0.20	−0.08

[a] Chemical shifts for free **1–6** (no DNA) and the shifts induced (Δδ) on addition of DNA to a ratio of 0.3 (compound to DNA base pairs). Experiments were conducted in phosphate–EDTA buffer at 65 °C. See Figure 1 for aromatic proton assignments; H2″ and H3″ refer to side-chain protons.

higher in energy. We thus expect **4**, as with **8**, to have a twist angle between ring planes of approximately 10° depending on conditions.

Finally, it should be noted that **3–8** can exist in the s-cis conformation (as shown in Figure 1) or in the s-trans orientation. Crystallographic and NMR NOE experiments indicate that the s-cis conformation is strongly preferred for the pyrimidine–thiophene systems (Strekowski et al., 1986a,b, 1988a). Molecular mechanics calculations on **3–8** support these experimental findings.

Mode of Binding. (*a*) *Viscometric Titrations.* The viscosity of sonicated calf thymus DNA is significantly increased by **1** and **3–6** but not by **2**, as can be seen in Figure 2. The maximum η/η_0 produced by **3–6** is in the range typically seen for intercalators (1.9 ± 0.3) (Waring, 1981; Wilson & Jones, 1981), but the increase for **1** is significantly below this range. The results with **2** are characteristic of a groove-binding mechanism (Waring, 1981; Zimmer & Wahnert, 1986).

The effects of ethidium and **3–5** on the viscosity of supercoiled DNA are shown in Figure 3. These titrations were repeated at several DNA concentrations, and the unwinding angles, determined by the Vinograd method (Revet et al., 1971; Jones et al., 1980), are 17°, 10°, and 19° for **3**, **4**, and **5**, respectively. Of the compounds **1–6**, only **2** does not give the characteristic viscosity increase, maximum, and decrease characteristic of intercalators (Waring, 1981; Wilson & Jones, 1981). The unwinding angle for **1** is 8° (Wilson et al., 1988). The 17–19° unwinding angles observed for **3** and **5** are in the range expected for a classical intercalation model (Wilson & Jones, 1981). The 10° value observed with **4** is quite low, and the viscosity increase observed with sonicated DNA on addition of **4** is also smaller than with **3**, **5**, and **6**. These results suggest that **4**, as observed with **1** (Wilson et al., 1988) does not form a typical intercalation complex with DNA.

(*b*) *NMR Studies.* The ^1H NMR assignments for **1–6** (Table I) were determined by analysis of chemical shifts, coupling constants, and NOE results (Wilson et al., 1988). NOE experiments also demonstrated that the ring systems of **3–6** have the s-cis equilibrium conformation in solution. The H5 protons of free **5** and **6** (Figure 1) at 65 °C, for example, have strong NOE cross peaks with H3′ of each compound, which are similar in intensity to the H3′–H4′ cross peaks.

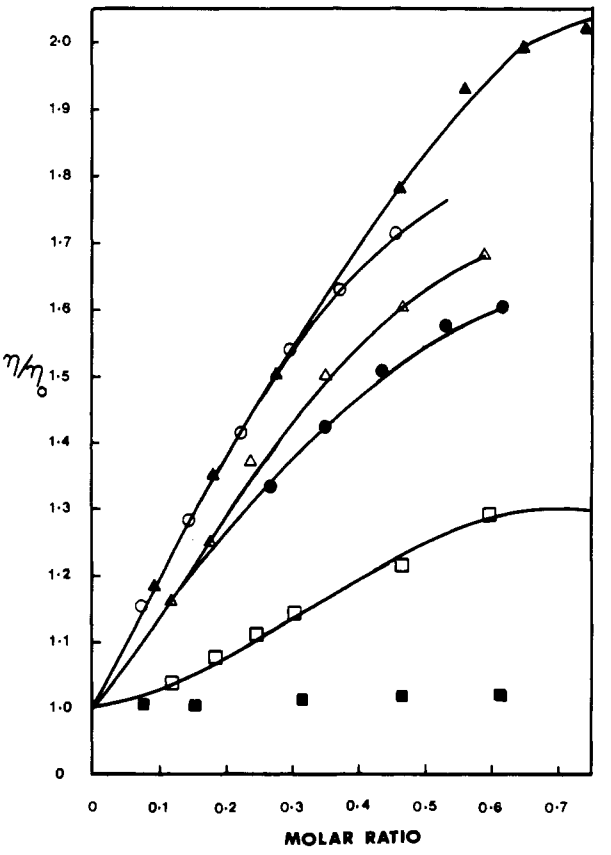

FIGURE 2: Viscosity increases of sonicated calf thymus DNA on addition of **3–6**. Viscometric titrations for **1** and **2** from Wilson et al. (1988) are included for reference: (□) **1**; (■) **2**; (○) **3**; (●) **4**; (▲) **5**; (△) **6**. The reduced specific viscosity ratio is plotted as a function of the molar ratio of compound to DNA base pairs. Experiments were conducted in PIPES 00 buffer at 31 °C at DNA concentrations near 1×10^{-4} M base pairs.

Similarly, the H3(4) proton in **3** has an intense NOE cross peak with H5′. Similar results have been found for **7**, the bicyclic analogue of **5** (Strekowski et al., 1986a).

Changes in chemical shifts for the aromatic protons of **6** on addition of DNA are shown, as an example for all compounds, in Figure 4, and proton chemical shift changes in the

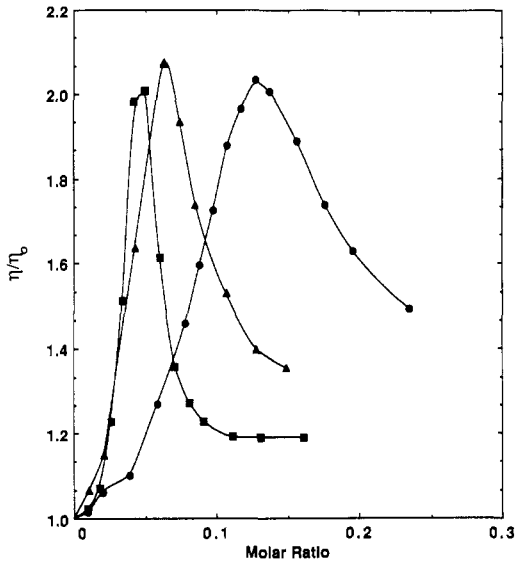

FIGURE 3: Visometric titrations of closed circular supercoiled DNA with (■) ethidium, (●) **4**, and (▲) **5**. Other compounds gave similar titrations but are not shown because of overlapping curves. Experiments were conducted in PIPES 00 buffer at 31 °C.

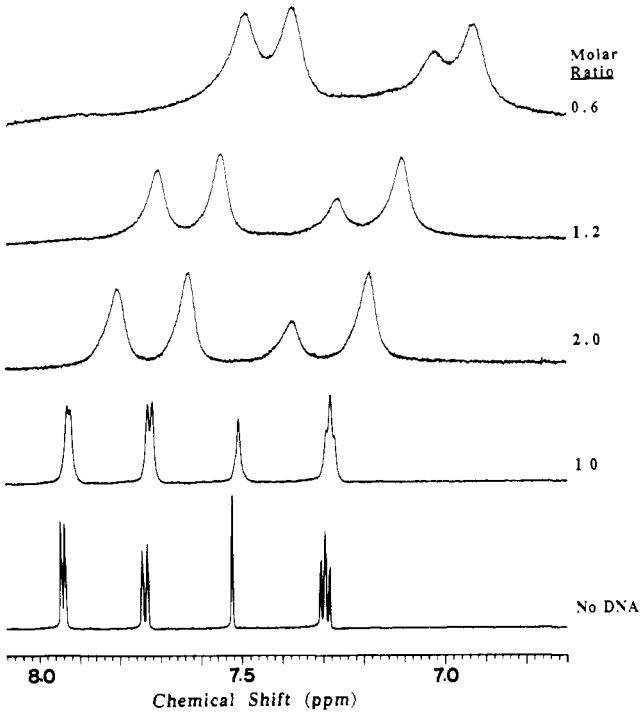

FIGURE 4: Proton NMR spectra in the aromatic proton region for **6** are shown as a function of the molar ratio (compound/base pair) of added sonicated calf thymus DNA. Experiments were conducted in phosphate–EDTA buffer at 65 °C at a final DNA concentration of 2 mM base pairs.

aromatic region for all compounds are collected in Table I. As can be seen, the aromatic protons of **1** and **3–6** shift significantly upfield on addition of DNA. The high temperature promotes exchange of the small molecules and results in significant sharpening of the NMR signals. DNA imino proton signals shift upfield and DNA phosphorus signals shift downfield when **1** and **3–6** are added to DNA (not shown). Compound **2** does not induce a significant shift in DNA imino proton or DNA phosphorus signals, and no significant shifts of the aromatic protons of **2** are seen when excess DNA is added (Table I). Compounds **1** and **3–6** all induce a 0.2–0.4 ppm upfield shift in the DNA imino proton signals. **1**, **3**, and **4** cause an approximately 0.2 ppm and **5** and **6** an approximately 0.4 ppm downfield shift in the DNA ^{31}P NMR signal (not shown).

Table II: Flow Dichroism Results[a]

compd	buffer	λ (nm)	^{red}D	λ (nm)	^{red}D
none	PIPES 00	260	−0.133		
	PIPES 20	260	−0.135		
1	PIPES 00	260	−0.075	330	−0.051
	PIPES 20	260	−0.129	330	−0.082
2	PIPES 00	260	−0.110	305	+0.002
	PIPES 20	260	−0.127	305	+0.002
3	PIPES 00	260	−0.072	367	−0.066
	PIPES 20	260	−0.123	367	−0.098
4	PIPES 00	260	−0.068	370	−0.062
	PIPES 20	260	−0.118	370	−0.094
5	PIPES 00	260	−0.132	353	−0.110
	PIPES 20	260	−0.132	353	−0.118
6	PIPES 00	260	−0.135	365	−0.135
	PIPES 20	260	−0.129	365	−0.110
propidium	PIPES 00	260	−0.120	520	−0.162
	PIPES 20	260	−0.136	520	−0.178
distamycin	PIPES 00	260	−0.064	320	+0.064
	PIPES 20	260	−0.116	320	+0.106

[a] Flow dichroism results (^{red}D) are given at the DNA maximum wavelength (260 nm) and at the bound ligand maximum wavelength in two buffers.

It is interesting to note that the aromatic protons on the center ring of each tricyclic intercalator experience the greatest upfield shifts in the presence of excess DNA. For example, H2 and H5 of **1** shift upfield 0.51 and 0.48 ppm, respectively, while H2′, H6′, H3′, and H5′ shift upfield 0.41 ppm. Also, H5 of **5** shifts upfield by 0.90 ppm while H5′ shifts only 0.56 ppm. Similarly, H3 and H4 of **3** shift upfield by 0.76 ppm while H6′ shifts only 0.47 ppm. In the monocationic intercalator group (**5** and **6**) the 3′ protons experience the next greatest upfield shifts (−0.75 ppm for H3′ of **5** and **6**). It should also be noted that the side-chain orientation on DNA in the intercalation complex with the monocations **5** and **6** is probably different from that of the two side chains in the complex with **1**, **3**, and **4**. For example, no significant shifts of the methylene (2″, 3″) or $N(CH_3)$ protons of **1–4** are seen on addition of DNA, but the methylenes of **5** and **6** exhibit a 0.2–0.3 ppm upfield shift and the $N(CH_3)$ protons shift upfield 0.07–0.09 ppm.

(*c*) *Flow Dichroism.* Flow dichroism studies on DNA alone and complexed with **1–6** were conducted at 260 nm, where absorption due to DNA dominates, and at the maximum wavelength above 300 nm of **1–6** in their DNA complexes. The results are collected in Table II and are compared to the phenanthridium intercalator, propidium, and the minor groove binding compound distamycin. Calf thymus DNA alone and complexed with **1**, **3–6**, and propidium exhibits a significant negative reduced dichroism (^{red}D) at 260 nm and at the maximum wavelength of the complex above 300 nm. Distamycin and **2** exhibit negative ^{red}D values at 260 nm but have positive ^{red}D values above 300 nm, where only the induced dichroism of the bound molecule is being monitored. The positive dichroism of distamycin is significantly larger than ^{red}D for **2**. In flow dichroism experiments in the low-salt PIPES 00 buffer, the monocations **5** and **6** had ^{red}D values that are similar to the values observed at high salt but the dications, **1**, **3**, and **4**, had lower ^{red}D values, suggesting that they exhibit some outside binding at low salt concentrations. The decrease in ^{red}D for the dication propidium was much less at low salt than for **1**, **3**, and **4**, suggesting that propidium has a significantly lower tendency to bind to DNA in an external mode.

Effect of Structure on Binding Strength and Specificity. (*a*) *Spectrophotometric Changes.* Addition of DNA to **1–6**

Table III: Binding Specificity Results

compd	calf thymus DNA			$d(A\text{-}T)_2$		$d(G\text{-}C)_2$		
	K_T[a]	$K \times 10^{-3}$ (M^{-1})	n	$K \times 10^{-3}$ (M^{-1})	n	$K \times 10^{-3}$ (M^{-1})	n	K_{AT}/K_{GC}
1[b]	160	13.3	3.3	86.5	3.7	7.2	>5[d]	12
2[c]	4	27.7	3.5	73.1	3.4	17.6	3.0	4.2
3[b]	2000	140.2	3.1	228.4	3.1	840	2.8	0.27
4[b]	1300	74.4	3.2					
5[b]	2500	27.4	2.3	144.4	2.0	8.8	~4[d]	16.5
6[b]	800	10.0	~4[d]					
quinacrine[e]	1300							
ethidium[e]	16000							

[a] K_T values were calculated with eq 2 at 1 M Na^+ from the results in Figure 7. [b] The experiments for **1** and **3–6** were conducted in a PIPES 10 buffer at 25 °C. [c] The studies with **2** were conducted in a PIPES 00 buffer. Binding of this compound to DNA in PIPES 10 was too weak for accurate analysis. The K_T value for this compound is estimated by assuming a slope of 2 in Figure 7. [d] The weak binding of these compounds made an accurate determination of n impossible. [e] Values calculated from results of Wilson et al. (1985a).

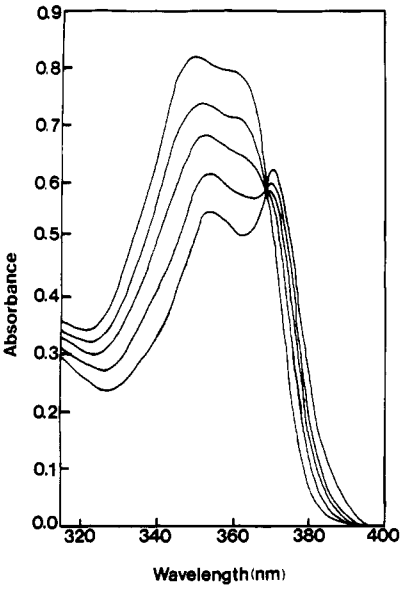

FIGURE 5: Spectral shifts in the visible adsorption region on addition of calf thymus DNA to **5**. The titration was conducted in a 1-cm cuvette at 25 °C in PIPES 00 buffer at a concentration of **5** of 3.7 × 10^{-5} M. The DNA concentration ranged from zero (top curve at 350 nm) to 2 × 10^{-4} M base pairs (bottom curve at 350 nm).

causes hypochromic changes and spectral shifts to longer wavelength for all compounds. Spectrophotometric titrations of **1** and **2** have been previously presented (Wilson et al., 1988), and a titration of **5** with DNA is shown in Figure 5, as an example of the pyrimidine–thiophene type compounds. In low ionic strength buffer (PIPES 00) at compound concentrations significantly above 1 × 10^{-5} M, isosbestic points were not obtained, particularly with the dications, in the titrations with DNA. At concentrations below 1 × 10^{-5} M in PIPES 00 (long path length cells) or at higher ionic strengths, isosbestic points were obtained (Figure 5). In agreement with flow dichroism studies, these results suggest that both intercalation and outside binding modes may occur at low ionic strength but that only intercalation binding is significant at higher ionic strengths. Bound extinction coefficients were determined at the same wavelength as the free extinction coefficients for use in calculating binding constants.

Results presented above have demonstrated that **2** does not intercalate. Titration of **2** with DNA, however, results in significant hypochromicity and spectral shifts to longer wavelength as with the intercalators **1** and **3–6**. This illustrates that absorption spectral changes are not definitive for making conclusions about the mode of binding of compounds to DNA.

(*b*) *Binding Strength.* Compounds **1–6** were titrated into DNA at a range of concentrations, and the free and bound

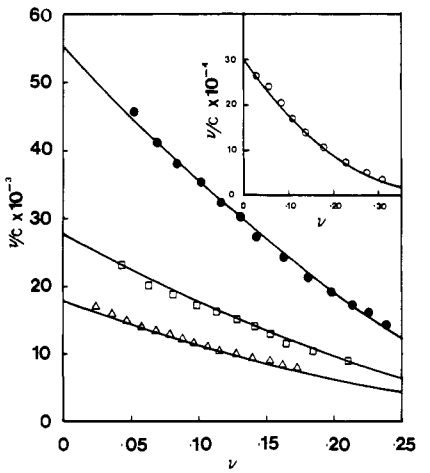

FIGURE 6: Scatchard plots for binding of **5** to calf thymus DNA in PIPES 00 (○), PIPES 05 (●), PIPES 10 (□), and PIPES 15 (△) buffers at 25 °C. Points in the figure are experimental, and the solid lines are from nonlinear least-squares best-fit values from eq 1.

extinction coefficients were used to construct binding isotherms (Wilson et al., 1985a). Isotherms in the form of Scatchard plots are shown at several ionic strengths for **5** in Figure 6. The points in the figure are experimental, and the solid lines are determined by a nonlinear least-squares computer program using the site exclusion model of McGhee and von Hippel (1979):

$$\nu/C = K[1 - n\nu][(1 - n\nu)/(1 - (n - 1)\nu)]^{n-1} \quad (1)$$

where ν is the moles of compound bound per DNA base pair, C is the free compound molarity, K is the observed binding equilibrium constant, and n is the number of base pairs per binding site. Binding constants for all compounds are given in Table III.

Using binding isotherms of the type shown in Figure 6, the equilibrium binding constants for **1** and **3–6** with calf thymus DNA were determined at several salt concentrations and are plotted according to eq 2 in Figure 7 (Record et al., 1978; Wilson et al., 1985a; Lohman, 1985). The slope for dication compounds **1**, **3**, and **4** is 1.9 ± 0.1, and the slope for monocation compounds **5** and **6** is 1.1 ± 0.1. The slopes for the dications are approximately twice the slope for monocations, as would be expected from their charges (Wilson et al., 1985a,b; Wilson & Lopp, 1979), and the values are in the range predicted for dications and monocations:

$$\log K_{obs} = \log K_T + m'\xi^{-1} \ln (\gamma_{\pm}\delta) - [2N(\Psi - \Psi^*) + m'\Psi^*] \log [Na^+] \quad (2)$$

where K_{obs} is the observed equilibrium constant at any salt

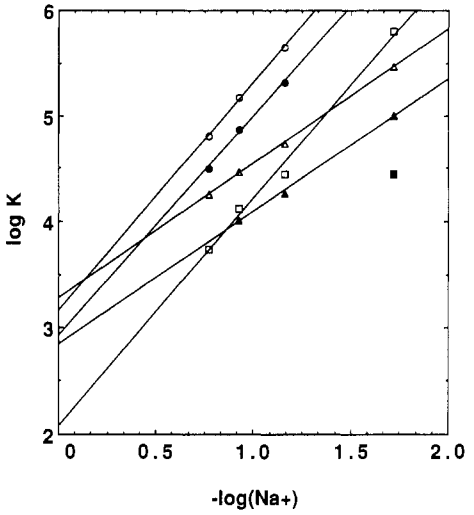

FIGURE 7: Plots of log K, the observed equilibrium constant, determined as in Figure 6 vs −log [Na^+]: (□) **1**; (■) **2**; (○) **3**; (●) **4**; (△) **5**; (▲) **6**. Results for **1** and **2** are from Wilson et al. (1988) and are included for reference. The solid lines are linear least-squares best-fit values according to eq 2.

concentration, K_T is the thermodynamic binding constant, N is the number of base pairs involved in the binding site, m' is the number of ion pairs in the complex (for small molecules, this usually equals the charge), $\Psi = \Psi_c + \Psi_s$ and $\Psi^* = \Psi_c^* + \Psi_s^*$, where Ψ_c and Ψ_c^* are the counterion fractions condensed on native and open DNA, respectively. Ψ_s and Ψ_s^* represent counterions per phosphate associated with DNA in a Debye–Hückel-type process (Wilson et al., 1985a). The second term is small and represents a correction for solution nonideality: $\gamma_\pm$ is the mean ion activity coefficient, and δ is a constant containing terms from the Debye–Hückel theory (Record et al., 1978). The term $-2N(\Psi - \Psi^*)$ comes from ion release from the DNA due to the intercalation-induced conformational change in DNA, and the term $m'\Psi^*$ results from ion release on intercalator binding to the open DNA (Wilson & Lopp, 1979; Wilson et al., 1985a,b). K_T values for **1** and **3–6**, determined by fitting the plots in Figure 7 with eq 2, are collected in Table III and are compared to values for the dicationic intercalator quinacrine and the monocationic intercalator ethidium.

(*c*) *Binding Specificity*. Scatchard binding isotherms were also determined for the binding of **1–3**, and **5** to synthetic DNA polymers. Example plots for the binding of **5** to all of the DNA samples are shown in Figure 8. The points in the figure are experimental, and the solid lines were determined as discussed above. The K and n values for the compounds determined in this manner are collected in Table III. With compounds **1**, **2**, and **5**, the highest binding constants are seen with poly[d(A-T)]·poly[d(A-T)] and the lowest binding constant with poly[d(G-C)]·poly[d(G-C)]. Compound **3** has the highest binding constant with poly[d(G-C)]·poly[d(G-C)] and the lowest with CT DNA. The preference of **5** for A·T base pairs is greater than the A·T preference of **1** and **2** as can be seen from the K_{AT}/K_{GC} ratios in Table III.

Discussion

Viscosity, flow dichroism, and NMR measurements provide different types of information about the binding mode of compounds that interact with DNA (Waring, 1981; Wilson & Jones, 1981; Bloomfield et al., 1974; Wilson, 1989). For linear DNA, the viscosity increases significantly for intercalation but increases much less or decreases for groove-binding molecules. With supercoiled DNA intercalators give a

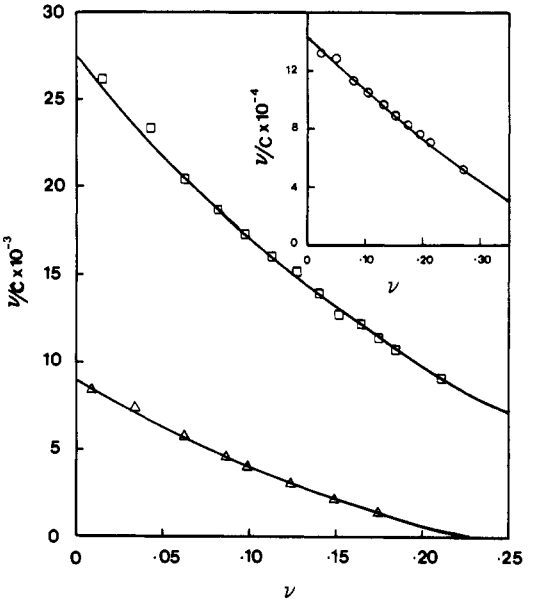

FIGURE 8: Scatchard plots for binding of **5** to d(A-T)$_2$ (○), calf thymus DNA (□), and d(G-C)$_2$ (△) in PIPES 10 buffer at 25 °C. Points in the figure are experimental, and the solid lines are results from nonlinear least-squares best-fit values from eq 1.

characteristic viscosity increase, maximum, and viscosity decrease as the intercalator is added to the DNA. Flow dichroism is negative and similar in magnitude to the dichroism for DNA base pairs for intercalators but can be zero or positive for groove-binding molecules. DNA imino proton signals shift upfield for intercalation but may not shift or may shift downfield for groove-binding interactions. DNA ^{31}P chemical shifts are downfield for intercalation but generally show no shift or an upfield shift for groove-binding molecules. Aromatic protons of an intercalator shift upfield under the influence of the ring current of the DNA base pairs, but aromatic protons on groove-binding molecules shift much less and may shift downfield.

Analysis of the DNA complexes of **1–6** with the above criteria clearly demonstrates that **1** and **3–6** are intercalators, while **2** does not intercalate. Compound **2** has the lowest binding constant of the six molecules and clearly forms the weakest interactions with DNA (Table III). The twist induced in the unfused aromatic rings of **2** by the pyrimidine methyl substituent must prevent formation of an intercalation complex. The interactions of **2** with DNA are, however, weaker than those of its closely related analogue **1**. The interaction of **2** with DNA is also significantly weaker than for the monocationic intercalators **5** and **6**. Obviously the twist of this molecule is not optimized to give an optimum complex in either of the grooves of DNA.

Comparison of the physical properties of the complexes of the intercalators **1** and **3–6** with DNA reveals some significant differences. The viscosity increase and the ^{red}D are largest for **5** and smallest for **1**. In the same manner the upfield shift of the H5 of the pyrimidine ring of **5** on addition of DNA is −0.90 ppm, while the same proton in **1** shifts upfield only −0.51 ppm. Chemical shift changes for the central ring protons of **3** and **4** are intermediate.

Extrapolation of the results of Figure 7 to 1.0 M NaCl allows comparison of binding constants in a standard state (eq 2). At the 1.0 M NaCl standard-state conditions, the order of binding constants is as follows: **5 > 3 > 4 > 6 > 1 > 2** (Figure 7 and Table III). Under these conditions charge interactions and counterion release do not have a large influence on the binding constant, and it is the direct interactions

of the intercalator with DNA that contribute most to the binding constant. As with the hydrodynamic results, **5** has the largest and **1** has the smallest thermodynamic binding constant for the intercalators. Extrapolation of the low-salt binding constant of **2** to 1.0 M salt (Table III), using a slope of 2, since it is a dication, indicates that under the high-salt conditions it would have a thermodynamic binding constant of less than 10. This again indicates that the interactions of **2** with DNA are largely electrostatic in nature and at low ionic strength are favorable primarily through counterion release.

At lower salt concentrations ion release makes a larger contribution to the observed equilibrium constant and at 0.1 M Na^+, for example, the order of observed binding constants is **3** > **4** > **5** > **1** > **6** > **2** (Figure 7). In comparing binding constants of a series of compounds to DNA, it is obviously essential to do so through a plot such as the one shown in Figure 7 if the compounds have different charges or differences in ion release due to other factors such as significant conformational differences in the complex with DNA.

The differences in the interactions of **1**–**6** with DNA can be understood from the structural, binding, hydrodynamic, and spectroscopic results reported here. At low salt concentrations there is an electrostatic contribution to binding (ion release) that is more favorable for the dications than for the monocations. This electrostatic interaction is less important as the salt concentration increases. Compound **2** has a very large intrinsic propeller twist and cannot stack well with DNA base pairs in an intercalation complex. It binds weakly to DNA in a relatively nonselective manner, probably in the major groove, at low salt concentration and dissociates from DNA at high salt. Compound **1** is also twisted, but significantly less than **2**, and can form an intercalation complex. Of the intercalators **1** and **3**–**6**, compound **1** causes the smallest increase in sonicated DNA viscosity and exhibits relatively small upfield proton NMR shift changes on complex formation. The reduced dichroism value is also relatively small for this compound, and all results taken together suggest that **1** must cause a distortion of DNA at the intercalation site. The intrinsic twist of **1** is obviously accomodated into the double-helix base-pair stack, but the base-pair twist is not exactly complementary to the twist for **1** and a distortion of DNA occurs on complex formation.

Both X-ray crystallographic and model calculations predict that **5** and **6** are planar. These molecules give large increases in linear DNA viscosity, they have large ^{red}D values, and they have large induced chemical shift changes in NMR titrations with DNA. Dipole moment considerations (Strekowski et al., 1986a; 1988a) predict that **5** should interact more strongly with DNA than **6** and this is observed. Both of these molecules interact quite well with DNA base pairs in an intercalation complex and cause minimal distortion of DNA at the intercalation site.

The pair of bis(pyrimidine) compounds **3** and **4** exhibit very interesting behavior that is between that observed for **1** and for **5** and **6**. On the basis of hydrodynamic and NMR results, it is clear that both **3** and **4** intercalate. The binding constant, linear viscosity, intercalation unwinding angle, and induced proton NMR shifts on addition of DNA are all significantly greater for **3** than for **4**. Model calculations indicate that **3** can easily adopt a planar conformation. This molecule can thus bind tightly to DNA with minimal distortion of the double helix. Crystallographic results for **8**, the bicyclic analogue of **4**, however, predict a twist between the pyrimidine and thiophene rings of 5–8°. For comparison the predicted twists for **1** and **2** are approximately 20° and 50°, respectively. With both viscosity and NMR results, **4** gives changes that fall between those observed for **1** and **3**. All three of these dications form two ion-pair interactions with DNA from slopes of log K vs $-\log [Na^+]$ plots (Figure 7). The binding strength of **4** is again intermediate, being less than for **3** but significantly greater than for **1**. All of these results suggest that **4** can form an intercalation complex with DNA but, probably due to the intrinsic twist of the molecule, causes some distortion of the double helix at the intercalation site.

It is interesting to note that, unlike the tricyclic compounds, **8**, the bicyclic analogue of **4**, binds approximately 3 times more strongly to DNA than **7**, the bicyclic analogue of **3** (Strekowski et al., 1986b, 1988a). Crystallographic and modeling calculations indicate that **8** is twisted slightly, while **7** is planar. The bicyclic compounds, however, as with the DNA base-pair complex, have only one propeller-twisted ring intersection. With the tricyclic compounds there are two potential propeller-twisted bonds. These results suggest that **8** forms an intercalation complex that complements the base-pair propeller twist (Strekowski et al., 1986b). This compound has the strongest interaction with DNA in the series of bicyclic compounds that we have examined (Strekowski et al., 1988a). With the tricyclic compound **4**, however, the two torsional degrees of freedom do not match the base-pair propeller twist, and the binding constant is less than for **3**. In addition, viscosity results suggest that **4** causes some distortion of the double helix on complex formation. Two important conclusions arise from these results. First, in designing intercalators to match or enhance base-pair propeller twist, it is better to work with compounds with only one torsional degree of freedom in the aromatic ring system. Second, in designing compounds to cause structural distortions, such as bends or kinks, in the DNA double helix, intercalators with two (or more) torsional degrees of freedom are preferred.

Perhaps the most surprising result with compounds **1**–**6** is the fact that the unfused aromatic cations **1** and **3**–**6** form strong intercalation complexes with DNA unlike structurally similar groove-binding compounds such as DAPI (**9** in Figure 1). We designed this series of compounds to probe the DNA interactions of unfused ring systems and to evaluate binding strength and specificity differences in intercalation versus groove-binding molecules of very similar nature. On the basis of other studies with unfused aromatic dications, we felt that **1**, **2**, and **4** had a high probability for being groove-binding molecules. Only with **2** did this prediction turn out to be correct. Clearly significant twist can be accommodated in an intercalation complex, and the differences between intercalation and groove-binding modes are more subtle than previously realized (Wilson, 1989). It appears that intercalation and groove-binding modes should be viewed as two variable-depth potential wells on a continuous energy surface. We are continuing to investigate the factors that influence the relative depths of the two wells.

References

Banville, D. B., Marzilli, L. G., Strickland, J. A., & Wilson, W. D. (1986) *Biopolymers 25*, 1837–1858.

Bloomfield, V. A., Crothers, D. M., & Tinoco, I. (1974) *Physical Chemistry of Nucleic Acids*, Harper and Row, New York.

Brown, D. J., & Grigg, G. W. (1982) *Med. Res. Rev. 2*, 193.

Brown, D. J., Cowden, W. B., & Strekowski, L. (1982) *Aust. J. Chem. 35*, 1209.

Burket, U., & Allinger, N. L. (1982) *Molecular Mechanics*, American Chemical Society, Washington, DC.

Calladine, C. R. (1982) *J. Mol. Biol. 161*, 343–352.

Clark, T. (1985) *A Handbook of Computational Chemistry*, Wiley, New York.
d'Annibale, A., Lunnazzi, L., Boicelli, A. C., & Macciantelli, D. (1973) *J. Chem. Soc., Perkin Trans. 2*, 1396–1400.
Dickerson, R. E. (1983) *J. Mol. Biol. 166*, 419–441.
Field, L. D., & Sternhell, S. (1981) *J. Am. Chem. Soc. 103*, 738–741.
Field, L. D., Sternhell, S., & Tracey, A. S. (1977) *J. Am. Chem. Soc. 99*, 5249–5253.
Ginell, S., Lessinger, L., & Berman, H. M. (1988) *Biopolymers 27*, 843–864.
Goodsell, D., & Dickerson, R. E. (1986) *J. Med. Chem. 29*, 727–733.
Hargraves, A., & Hasan-Rizvi, S. (1962) *Acta Crystallogr. 15*, 365–373.
Helene, C., Montenay-Garestier, T., Saison, T., Takasugi, M., Toulme, J. J., Aseline, U., Lancelot, G., Maurizot, J. C., Toulme, F., & Thuong, N. T. (1985) *Biochimie 67*, 777–783.
Hurley, L. H., & Boyd, F. L. (1987) *Annu. Rep. Med. Chem. 22*, 259–268.
Jones, R. L., Lanier, A. C., Keel, R. A., & Wilson, W. D. (1980) *Nucleic Acids Res. 8*, 1613–1624.
Laugaa, D., Markovits, J., Delbarre, A., Le Pecq, J.-B., & Roques, B. P. (1985) *Biochemistry 24*, 5567–5575.
Lee, M., Hartley, J. A., Pon, R. T., Krowicki, K., & Lown, J. W. (1988) *Nucleic Acids Res. 16*, 665–684.
Lohman, T. (1985) *CRC Crit. Rev. Biochem. 19*, 191–245.
McGhee, J. D., & von Hippel, P. H. (1974) *J. Mol. Biol. 86*, 469–489.
Moser, H. E., & Dervan, P. B. (1987) *Science 238*, 645–650.
Palmer, B. D., Rewcastle, G. W., Atwell, G. J., Baguley, B., & Denny, W. A. (1988) *J. Med. Chem. 31*, 707–712.
Pullman, B. (1987) in *Structure and Expression* (Sarma, R. H., & Sarma, M. H., Eds.) Vol. 2, pp 237–249, Adenine Press, New York.
Revet, B., Schmir, M., & Vinograd, J. (1971) *Nature, New Biol. 229*, 10–14.
Sinton, S. W., Zax, D. B., Murdoch, J. B., & Pines, A. (1984) *Mol. Phys. 53*, 333–362.
Strekowski, L., Chandrasekaran, S., Wang, Y. H., Edwards, W. D., & Wilson, W. D. (1986a) *J. Med. Chem. 29*, 1311–1315.
Strekowski, L., Tanious, F. A., Chandrasekaran, S., Watson, R. A., & Wilson, W. D. (1986b) *Tetrahedron Lett. 27*, 6045.
Strekowski, L., Strekowska, A., Watson, R. A., Tanious, F. A., Nguyen, L. J., & Wilson, W. D. (1987) *J. Med. Chem. 30*, 1415–1420.
Strekowski, L., Mokrosz, J. L., Tanious, F. A., Watson, R. A., Harden, D., Mokrosz, M., Edwards, W. D., & Wilson, W. D. (1988a) *J. Med. Chem. 31*, 1231.
Strekowski, L., Wilson, W. D., Mokrosz, J. L., Strekowska, A., Koziol, A. E., & Palenik, C. J. (1988b) *Anti-Cancer Drug Des. 2*, 387–398.
Stubbe, J., & Kozarich, J. W. (1987) *Chem. Rev. 87*, 1107–1136.
Trotter, J. (1961) *Acta Crystallogr. 14*, 1135–1140.
Tung, C. S., & Harvey, S. C. (1986) *J. Biol. Chem. 261*, 3700–3709.
Wakelin, L. P. G. (1986) *Med. Res. Rev. 6*, 275–340.
Waring, M. (1981) in *The Molecular Basis of Antibiotic Action* (Gale, R., et al., Eds.) pp 314–333, Wiley, London.
Wilson, W. D. (1989) in *Nucleic Acids in Chemistry and Biology* (Blackburn, M., & Gait, M., Eds.) Chapter 8, IRL Press, Oxford, U.K. (in press).
Wilson, W. D., & Lopp, I. G. (1979) *Biopolymers 18*, 3025–3041.
Wilson, W. D., & Jones, R. L. (1981) *Adv. Pharmacol. Chemother. 18*, 177–222.
Wilson, W. D., Krishnamoorthy, C. R., Wang, Y. H., & Smith, J. C. (1985a) *Biopolymers 24*, 1941–1961.
Wilson, W. D., Wang, Y.-H., Kusuma, S., Chandrasekaran, S., Young, N. C., & Boykin, D. W. (1985b) *J. Am. Chem. Soc. 107*, 4989–4995.
Wilson, W. D., Strekowski, L., Tanious, F. A., Watson, R. A., Mokrosz, J. L., Strekowska, A., Webster, G. D., & Neidle, S. (1988) *J. Am. Chem. Soc. 110*, 8292–8299.
Zimmer, C., & Wahnert, U. (1986) *Prog. Biophys. Mol. Biol. 47*, 31–112.